

MiR-296-5p ameliorates deep venous thrombosis by inactivating S100A4

Zhichang Pan^{1,*}, Yu Zhang^{2,*}, Chuanyong Li¹, Yuan Yin³, Rui Liu⁴, Guangfeng Zheng¹, Weijian Fan¹, Qiang Zhang¹, Zhenyu Song¹, Ziyue Guo¹, Jianjie Rong¹  and Yixin Shen²

¹Department of Vascular Surgery, Suzhou TCM Hospital Affiliated to Nanjing University of Chinese Medicine, Suzhou 215000, China;

²Department of Orthopedics, The Second Affiliated Hospital of Soochow University, Suzhou 215006, China; ³Department of Endocrinology, Suzhou TCM Hospital Affiliated to Nanjing University of Chinese Medicine, Suzhou 215000, China; ⁴Department of Rheumatology, Suzhou TCM Hospital Affiliated to Nanjing University of Chinese Medicine, Suzhou 215000, China

Corresponding authors: Jianjie Rong. Email: vascularrijj@163.com; Yixin Shen. Email: 972679925@qq.com

*These authors contributed equally to this work.

Impact statement

Deep venous thrombosis (DVT) is one of the most common vascular diseases and a significant cause of morbidity and mortality worldwide. Therefore, understanding the pathogenesis of DVT and seeking promising diagnostic and therapeutic targets for DVT are important. Our study first demonstrates that miR-296-5p and S100A4 play important roles in the development of DVT and that targeting miR-296-5p or S100A4 could ameliorate DVT. Our research offers two potential therapeutic targets for DVT and explores the molecular mechanism of the miR-296-5p/S100A4 axis in DVT. These findings could lay a foundation for targeted therapy for DVT.

Abstract

Deep venous thrombosis is one of the most common venous thromboembolic diseases and has a low cure rate and a high postoperative recurrence rate. Furthermore, emerging evidence indicates that microRNAs are involved in deep venous thrombosis. miR-296-5p is an important microRNA that plays a critical role in various cellular functions, and S100A4 is closely related to vascular function. miR-296-5p is downregulated in deep venous thrombosis patients, and its predicted target S100A4 is upregulated in deep venous thrombosis patients. Therefore, it was hypothesized that miR-296-5p may play a vital role in the development of deep venous thrombosis by targeting S100A4. An Ox-LDL-stimulated HUVEC and deep venous thrombosis mouse model was employed to detect the biological functions of miR-296-5p and S100A4. Dual luciferase reporter assays and pull-down assays were used to authenticate the interaction between miR-296-5p and S100A4. ELISA and Western blotting were employed to detect the protein levels of thrombosis-related factors and the endothelial-to-mesenchymal transition (EndMT)-related factors. The miR-296-5p levels were reduced, while the S100A4 levels were enhanced in deep venous thrombosis patients, and the miR-296-5p levels were negatively correlated with the S100A4 levels in deep venous thrombosis patients. miR-296-5p suppressed S100A4 expression by targeting the 3' UTR of S100A4. MiR-296-5p knockdown accelerated ox-LDL-induced HUVEC apoptosis, oxidative stress, thrombosis-related factor expression, and EndMT, while S100A4 knockdown antagonized these effects in ox-LDL-induced HUVECs. S100A4 knockdown reversed the effect induced by miR-296-5p knockdown. Moreover, the *in vivo* studies revealed that miR-296-5p knockdown in deep venous thrombosis mice exacerbated deep venous thrombosis formation, whereas S100A4 knockdown had the opposite effect. These results indicate that elevated miR-296-5p inhibits deep venous thrombosis formation by inhibiting S100A4 expression. Both miR-296-5p and S100A4 may be potential diagnostic markers and therapeutic targets for deep venous thrombosis.

Keywords: Deep venous thrombosis, oxidative stress, EndMT, miR-296-5p, S100A4

Experimental Biology and Medicine 2021; 246: 2259–2268. DOI: 10.1177/15353702211023034

Introduction

Deep venous thrombosis (DVT) is a vascular disease and a significant cause of morbidity and mortality worldwide.¹ DVT formation is considered to be caused by three main

factors, including blood stagnancy, endothelial dysfunction, and hypercoagulability.^{2,3} Thrombolytics and interventional therapies are the major strategies applied for the treatment of DVT, but treated patients still have a low

cure rate and a high postoperative recurrence rate.⁴ Therefore, it is urgent to study the potential mechanisms of DVT and explore potential diagnostic and therapeutic targets.

MicroRNAs (miRNAs) are endogenous short noncoding RNAs that are approximately 21 to 24 nucleotides in length that play important roles in the regulation of gene expression.⁵ miRNAs are extensively implicated in physiological and pathological processes.⁶ Furthermore, miRNAs reportedly participate in the formation and development of DVT, providing promising new targets for the treatment of DVT.^{7,8} However, the roles of miR-296-5p in DVT are still unknown.

In the present study, we observed decreased miR-296-5p expression and increased S100A4 expression in DVT patients and investigated the regulatory mechanism between miR-296-5p and S100A4. An ox-LDL induced HUVEC injury and DVT mouse model was employed to investigate the functions of miR-296-5p and S100A4 *in vitro* and *in vivo*. The loss- and gain-of-function experiments proved the role of miR-296-5p and S100A4 in oxidative stress, the endothelial-to-mesenchymal transition (EndMT), and thrombosis-related factor release in DVT. Therefore, our results demonstrate that decreased miR-296-5p is implicated in DVT formation by inhibiting S100A4. miR-296-5p and S100A4 could act as diagnostic and therapeutic markers of DVT.

Materials and methods

Patients

Between May 2019 and December 2020, venous blood samples were collected from 41 DVT patients and 41 healthy controls. The DVT patients were verified by color Doppler ultrasound and lower extremity angiography and had no history of chronic diseases. The research was approved by the Ethics Committee of Suzhou TCM Hospital Affiliated to Nanjing University of Chinese Medicine. Written informed consent was obtained from each volunteer.

Cell culture

HUVECs were purchased from the American Type Culture Collection and cultured in DMEM (Invitrogen) with 10% fetal bovine serum (Invitrogen), 100 U/mL penicillin and 100 µg/mL streptomycin (Sigma-Aldrich). The cells were housed in a humidified atmosphere containing 5% CO₂ and cultured at 37°C. ox-LDL was obtained from YEASEN (Shanghai, China).

RNA isolation and quantification

miRNA was extracted from cells using a miRcute miRNA isolation kit (TIANGEN), and mRNA was extracted using TRIzol (Life Technologies). Then, the miRNA was reverse transcribed into cDNA using a TaqMan MicroRNA Assays Reverse Transcription kit (TIANGEN), and the mRNA was reverse transcribed to cDNA using a First-Strand Synthesis kit (Takara). A SYBR Premix Ex Taq kit (Takara) was used for the quantitative PCR (qPCR) analysis. The relative

expression was calculated using the $2^{-\Delta\Delta CT}$ method with normalization to GAPDH or U6. The primer sequences were as follows: miR-296-5p sense, 5'-TGCCTAATT CAGAGGGTTGG-3" and antisense, 5'-CTCCACTCCTGG CACACAG-3"; S100A4 sense, 5'-GATGAGCAACTTGG ACAGCAA-3' and antisense, 5'-CTGGGCTGCTTATCTG GGAAG-3'; GAPDH sense, 5'-AACTTTGGCATTGTGG AAGG-3" and antisense, 5'-ACACATTGGGGGTAGG AACA-3" ; and U6 sense, 5'-CTCGCTTCGGCAGCACACA-3" and antisense, 5'-ACGCTTCACGAATTTGCGT-3".

Western blot analysis

The proteins were isolated using RIPA reagent (Beyotime), and then, the concentration was quantified by a Pierce BCA Protein Assay Kit (Thermo Fisher Scientific). Thirty micrograms of protein were separated by 10% SDS-PAGE and transferred to polyvinylidene fluoride membranes (Millipore) after electrophoresis. After blocking with 5% skim milk, the membrane was incubated with primary antibodies against S100A4, CD31, α -SMA, vimentin, or GAPDH and incubated with a secondary antibody. The protein bands were visualized using enhanced chemiluminescence (Solarbio). All antibodies were purchased from Abcam.

Cell viability

Transfected HUVECs (30,000 per well) were exposed to ox-LDL (40 µg/mL) for 48 h, and then 10 µL of Cell Counting Kit-8 (Beyotime) were added. The absorbance was determined at 450 nm after all cells were incubated at 37°C for 2 h.

Cell apoptosis assay

The apoptosis assays were performed using an Annexin V-FITC/PI apoptosis detection kit (BD Biosciences). Briefly, the transfected HUVECs were exposed to ox-LDL (40 µg/mL) for 48 h, resuspended in binding buffer, and stained with 10 µL Annexin V-FITC and PI for 15 min in the dark. The apoptotic cells were analyzed by FlowJo software.

Dual luciferase reporter assay

WT or MUT S100A4 3'UTR containing miR-296-5p binding sequences was synthesized and cloned into the pmirGLO vector (Promega). HUVECs were cotransfected with the recombinant vector and miR-296-5p agomir for 48 h. A dual-luciferase reporter assay kit (Promega) was applied to detect luciferase activity. Renilla luciferase activity was used as the internal control.

Pull-down assay

The cells were lysed after cell cross-linking. Biotinylated miR-296-5p and nonspecified probes ordered from GenePharma were added to the cell lysates. All samples were incubated for 4–6 h at room temperature under moderate agitation. Dynabeads M-280 Streptavidin (Invitrogen) were added and incubated at 4°C overnight. Eluted RNAs

were analyzed by qRT-PCR after purification using an RNA purification kit (QIAGEN).

Intracellular ROS measurement

DCFH-DA (2',7'-dichlorodihydrofluorescein diacetate) (Sigma) was employed for the ROS detection. The treated HUVECs were stained with 20 μ M DCFH-DA for 30 min, and then the fluorescence intensity of the samples was analyzed by flow cytometry.

Evaluation of the malondialdehyde, superoxide dismutase, and nitric oxide levels

The levels of malondialdehyde (MDA), superoxide dismutase (SOD), and nitric oxide (NO) in the supernatants of the HUVECs were measured using a commercial MDA assay kit (AmyJet Scientific), SOD assay kit (AmyJet Scientific), and nitric oxide detection kit (AmyJet Scientific) following the kit protocols provided by the manufacturer.

ELISA

The concentrations of endothelin-1 (ET-1) and von Willebrand Factor (vWF) in the supernatants of the HUVECs were measured using ELISA kits (Abcam). A 6-keto-PGF1 α ELISA kit (Abcam) was employed to examine the levels of PGI2 in the supernatants.

DVT mouse model and treatment

C57BL/6J mice (age 8–12 weeks, male) were obtained from the SPF Biotechnology Company. The animal experiments were conducted in accordance with the guidelines for the Animal Research and Care Committee of Suzhou TCM Hospital Affiliated to Nanjing University of Chinese Medicine. DVT was induced by inferior vena cava (IVC) ligation.⁹ Briefly, the IVC was isolated and completely ligated at the level of the renal veins after anesthetization. The posterior branches were left open. The mice were sacrificed 24 h after the operation. The thrombi were excised and immediately weighed. Sections of the specimens 2 mm below the IVC ligation were fixed with 4% PFA for the hematoxylin and eosin (H&E) analysis. The negative control antagomir (antagomir-NC) or miR-296-5p antagomir (RiboBio) was administered at a dose of 10 nmol per mouse by tail intravenous injection. The lentiviral vector (LV) sh-S100A4 and its controls (GenePharma) were also administered by tail intravenous injection. All mice received the treatments two days before the IVC ligation and were sacrificed 24 h after the operation.

Statistical analysis

The data in this study are reported as the mean \pm standard deviation (SD) of three independent experiments. The differences were analyzed by Student's *t*-test or one-way analysis of variance (ANOVA). *P* < 0.05 indicates statistical significance.

Results

ox-LDL inhibits miR-296-5p levels in HUVECs

To investigate whether miR-296-5p is involved in HUVEC injury, cells were treated with ox-LDL at different concentrations (0–80 μ g/mL) for 48 h, and the miR-296-5p level was detected by RT-qPCR. As shown in Figure 1(a), ox-LDL decreased the miR-296-5p levels in a dose-dependent manner. Furthermore, we treated HUVECs with 40 μ g/mL ox-LDL for various durations (0–48 h) and found that ox-LDL downregulated miR-296-5p expression in a time-dependent manner (Figure 1(b)). To further study the role of miR-296-5p in ox-LDL-induced HUVEC injury, loss- and gain-of-function experiments were carried out. The miR-296-5p antagomir obviously downregulated the miR-296-5p levels in the HUVECs, and the miR-296-5p agomir obviously enhanced the miR-296-5p levels in the HUVECs (Figure 1(c) and (d)). In addition, we found that the miR-296-5p agomir reversed the suppression of HUVEC viability induced by ox-LDL, while the miR-296-5p antagomir further aggravated the suppression of HUVEC viability induced by ox-LDL (Figure 1(e)). Moreover, ox-LDL significantly promoted apoptosis in the HUVECs. The miR-296-5p agomir inhibited apoptosis, while the miR-296-5p antagomir enhanced apoptosis induced by ox-LDL (Figure 1(f)). These results show that miR-296-5p is involved in ox-LDL-induced HUVEC injury.

S100A4 is a direct target of miR-296-5p in HUVECs

To investigate the mechanism of miR-296-5p in HUVECs, the Encyclopedia of RNA Interactomes (ENCORI) was used to predict the putative targets of miR-296-5p. S100A4 plays a key role in cell function and may be a probable target gene of miR-296-5p. The binding sequences between miR-296-5p and S100A4 mRNA are shown in Figure 2(a). The luciferase assay indicated that reduced luciferase reporter activity was observed after the cotransfection of the luciferase reporter plasmid containing WT-S100A4 and miR-296-5p agomir in the HUVECs (Figure 2(b)). Moreover, a biotinylated pulldown assay was performed to confirm the interaction between miR-296-5p and S100A4 mRNA. S100A4 mRNA was detected in the fragments pulled down by biomiR-296-5p (Figure 2(c)). As shown in Figure 2(d), after the ox-LDL treatment, the protein level of S100A4 was enriched in the HUVECs. The miR-296-5p agomir notably reduced S100A4 protein expression, while the miR-296-5p antagomir enhanced S100A4 protein expression in the ox-LDL-treated HUVECs. These results suggest that miR-296-5p restrained S100A4 expression by targeting its 3'-UTR.

miR-296-5p/S100A4 axis affects ox-LDL-triggered oxidative stress

Subsequently, we explored the effect of the miR-296-5p/S100A4 axis on ox-LDL-triggered HUVEC injury. HUVECs cotransfected with miR-296-5p antagomir or sh-S100A4 were exposed to ox-LDL. As shown in Figure 3(a), the ox-LDL-elevated S100A4 expression was enhanced by the miR-

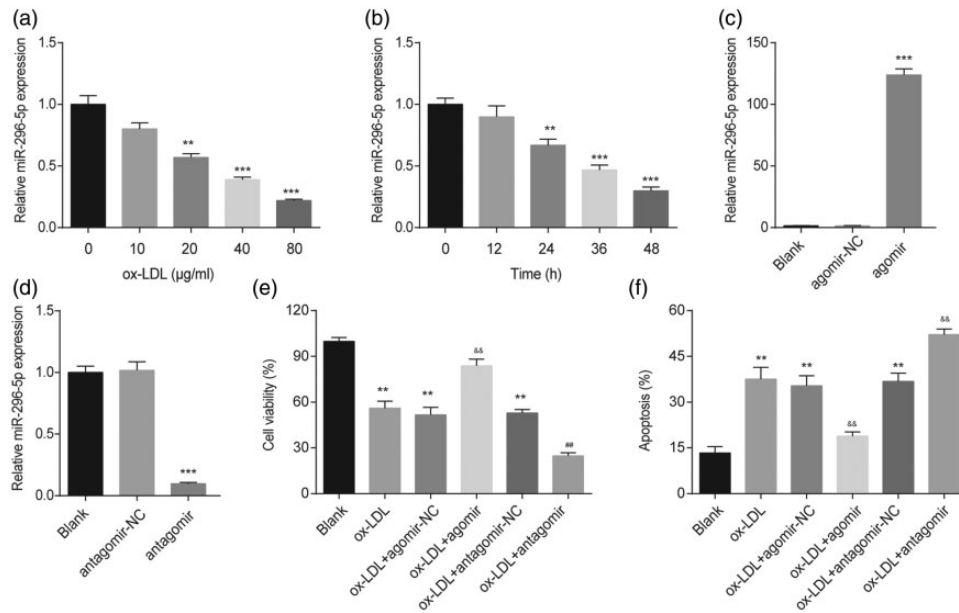


Figure 1. miR-296-5p was involved in ox-LDL-induced HUVEC injury. (a) miR-296-5p levels in HUVECs treated with ox-LDL at different concentrations (0, 10, 20, 40, or 80 µg/mL) for 48 h. $^{**}P < 0.01$, $^{***}P < 0.001$ vs. 0 µg/mL. (b) miR-296-5p levels in HUVECs treated with 40 µg/mL ox-LDL for various durations (0, 12, 24, or 48 h). $^{**}P < 0.01$, $^{***}P < 0.001$ vs. 0 h. (c) miR-296-5p levels in HUVECs transfected with the miR-296-5p agomir. $^{***}P < 0.001$ vs. agomir-NC. (d) miR-296-5p levels in HUVECs transfected with the miR-296-5p antagonist. $^{***}P < 0.001$ vs. antagonist-NC. (e) After transfection with the miR-296-5p agomir or miR-296-5p antagonist, HUVECs were treated with ox-LDL (40 µg/mL) for 48 h. A Cell Counting Kit-8 assay was used to detect the cell viability. $^{**}P < 0.001$ vs. Blank; $^{\&\&}P < 0.001$ vs. ox-LDL+ agomir-NC; $^{\#}P < 0.001$ vs. ox-LDL+ antagonist-NC. (f) Cell apoptosis was evaluated using flow cytometry. $^{**}P < 0.01$ vs. Blank; $^{\&\&}P < 0.01$ vs. ox-LDL+ agomir-NC; $^{\#}P < 0.01$ vs. ox-LDL+ antagonist-NC.

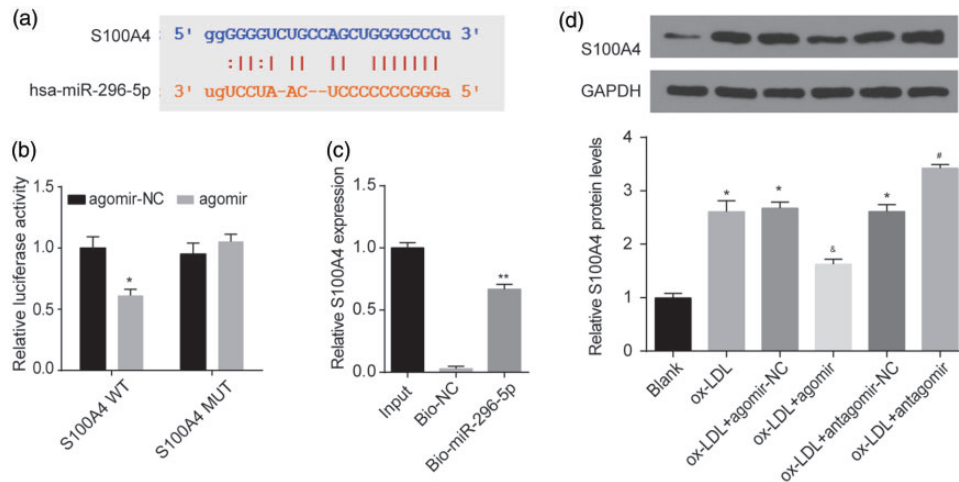


Figure 2. S100A4 acted as a direct target of miR-296-5p. (a) Complementary binding between miR-296-5p and the S100A4 3'UTR. (b) A dual-luciferase reporter assay verified the interaction between miR-296-5p and S100A4. $^{*}P < 0.05$ vs. agomir-NC. (c) S100A4 levels in samples pulled down using biotinylated miR-296-5p were detected by qRT-PCR. $^{**}P < 0.01$ vs. biotin-NC. (d) After the transfection with the miR-296-5p agomir or antagonist, HUVECs were exposed to ox-LDL (40 µg/mL) for 48 h, and then the S100A4 protein level was detected. $^{*}P < 0.05$ vs. Blank; $^{\&}P < 0.05$ vs. ox-LDL+ agomir-NC; $^{\#}P < 0.05$ vs. ox-LDL+ antagonist-NC. (A color version of this figure is available in the online journal.)

296-5p antagonist and was reduced by sh-S100A4. The miR-296-5p antagonist-induced upregulation of S100A4 protein was reversed by sh-S100A4. Furthermore, we found that S100A4 knockdown reversed the suppression of cell viability and the promotion of apoptosis induced by ox-LDL (Figure 3(b) and (c)). The S100A4 knockdown also alleviated the effects on cell viability and apoptosis induced by the miR-296-5p antagonist in the HUVECs following the ox-LDL treatment (Figure 3(b) and (c)).

We further explored the role of the miR-296-5p/S100A4 axis in ox-LDL-induced ROS in HUVECs. The ox-LDL treatment significantly increased the ROS levels in the HUVECs. As shown in Figure 3(d) and (e), the miR-296-5p antagonist markedly enhanced the ROS levels induced by ox-LDL, while the knockdown of S100A4 obviously reduced the ROS levels induced by ox-LDL. To explore the antioxidative roles of the miR-296-5p/S100A4 axis, we also detected the leakage of malondialdehyde (MDA) and

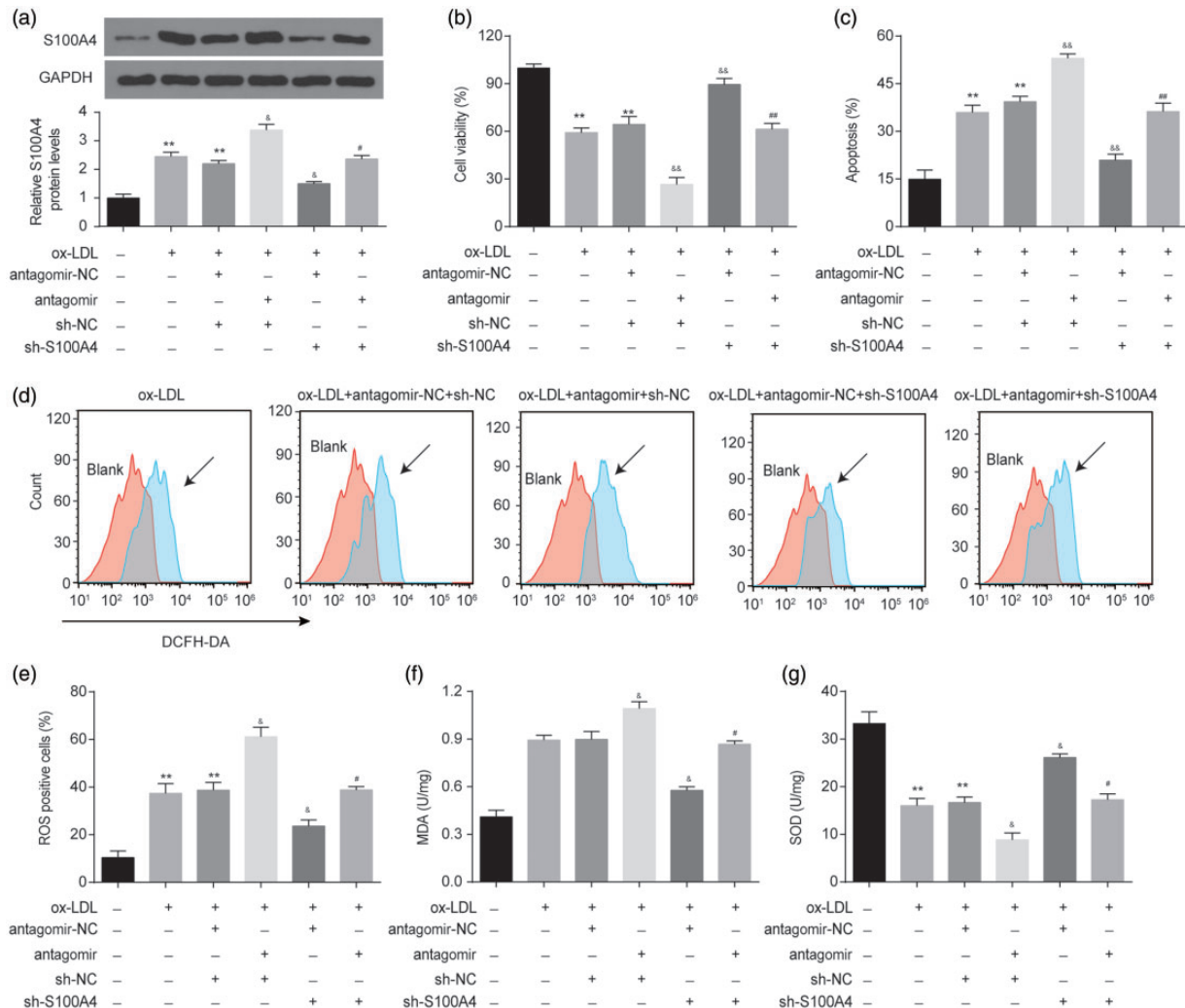


Figure 3. miR-296-5p restrains ox-LDL-induced oxidative stress injury in HUVECs through S100A4. After the transfection with the miR-296-5p antagonist or sh-S100A4, HUVECs were treated with ox-LDL (40 μ g/mL) for 48 h. (a) S100A4 protein was detected in HUVECs after the indicated treatment. (b) Cell viability was detected by a Cell Counting Kit-8 assay. (c) Cell apoptosis was evaluated using flow cytometry. (d–e) ROS levels were detected by DCFH-DA staining and then quantized by flow cytometry. (f–g) The generation of MDA and SOD was detected by ELISA. ** $P < 0.01$ vs. Blank; * $P < 0.05$, && $P < 0.01$ vs. ox-LDL+antagomir-NC+sh-NC; # $P < 0.05$, ## $P < 0.01$ vs. ox-LDL+antagomir+sh-NC. (A color version of this figure is available in the online journal.)

the production of superoxide dismutase (SOD) in HUVECs. As shown in Figure 3(f), the ox-LDL-elevated MDA leakage was enhanced in the miR-296-5p antagonist-pretreated groups and was inhibited in the S100A4 knockdown groups. Concomitantly, the miR-296-5p antagonist treatment enhanced the adverse impact of ox-LDL on SOD production, while the S100A4 knockdown improved the adverse impact of ox-LDL on SOD production (Figure 3(g)). Furthermore, the S100A4 knockdown restored the effects on ROS, MDA and SOD production induced by the miR-296-5p antagonist in the HUVECs following the ox-LDL treatment (Figure 3(d) to (g)). In short, the miR-296-5p/S100A4 axis alleviated ox-LDL-triggered oxidative stress injury in the HUVECs.

miR-296-5p/S100A4 axis improves thrombosis-related factor levels in HUVECs after ox-LDL treatment

Endothelial cell injury plays a vital role in thrombosis.¹⁰ Thus, we explored the effect of the miR-296-5p/S100A4

axis on thrombosis-related factor levels in HUVECs under ox-LDL stimulation. As shown in Figure 4(a) and (b), the miR-296-5p antagonist enhanced the ox-LDL-induced release of endothelin-1 (ET-1, a vital regulator of vasoconstriction) and von Willebrand factor (vWF, a prothrombotic risk factor) in HUVECs after the ox-LDL stimulation. The S100A4 knockdown inhibited the ox-LDL-induced release of ET-1 and vWF. In addition, we found that the miR-296-5p antagonist aggravated the adverse effects of ox-LDL on the vasodilatation-related factor nitric oxide (NO) and prostaglandin F1 α (PGF1 α) production, while the S100A4 knockdown reduced the adverse impact of ox-LDL on NO and PGF1 α production (Figure 4(c) and (d)). Furthermore, the S100A4 knockdown ameliorated the effect of the miR-296-5p antagonist on ET-1, vWF, NO, and PGF1 α production (Figure 4). In summary, the miR-296-5p/S100A4 axis was involved in the thrombosis-related factor levels in the HUVECs after the ox-LDL exposure.

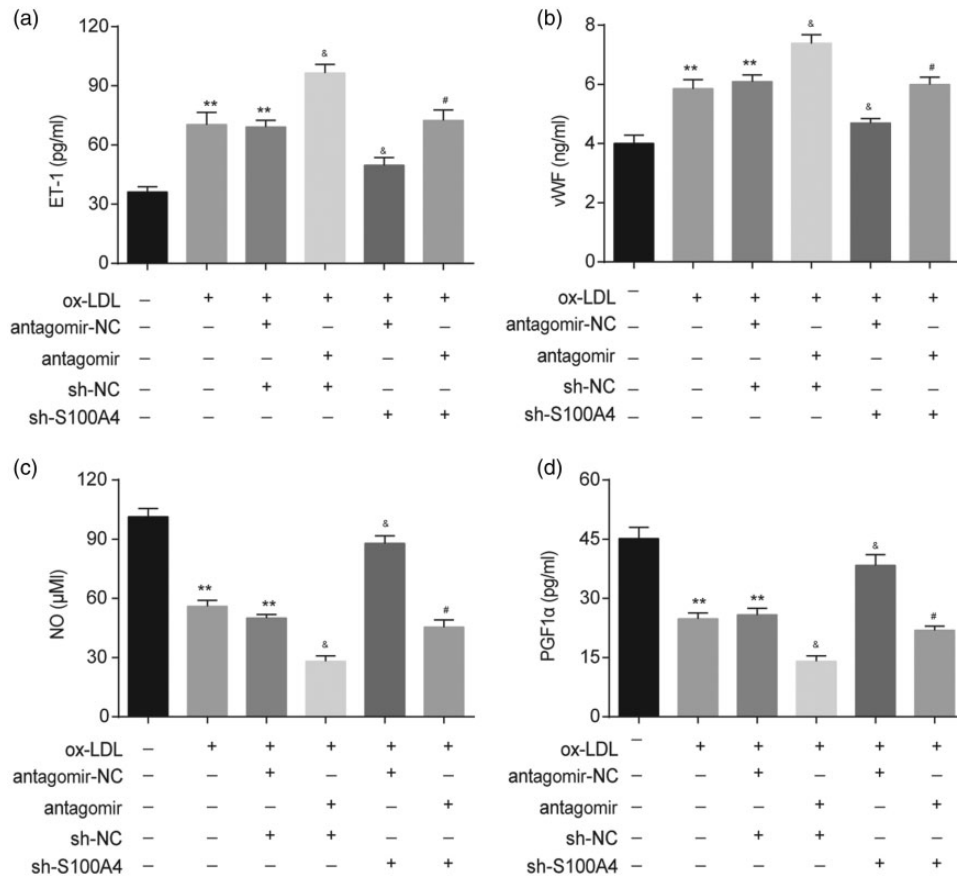


Figure 4. miR-296-5p/S100A4 axis was involved in thrombosis-related factor expression in HUVECs upon ox-LDL stimulation. After the transfection with the miR-296-5p antagonir or sh-S100A4, HUVECs were treated with ox-LDL (40 μg/mL) for 48 h. (a) The levels of ET-1 in the supernatants were detected by ELISA. (b) The generation of vWF was also assessed. (c) Generated NO was measured by the Griess reaction. (d) PGF1α production was analyzed by ELISA. ***P* < 0.01 vs. Blank; &*P* < 0.05 vs. ox-LDL+antagonir-NC+sh-NC; #*P* < 0.05 vs. ox-LDL+antagonir+sh-NC. Error bars show the SD derived from three replicate wells in the same plate.

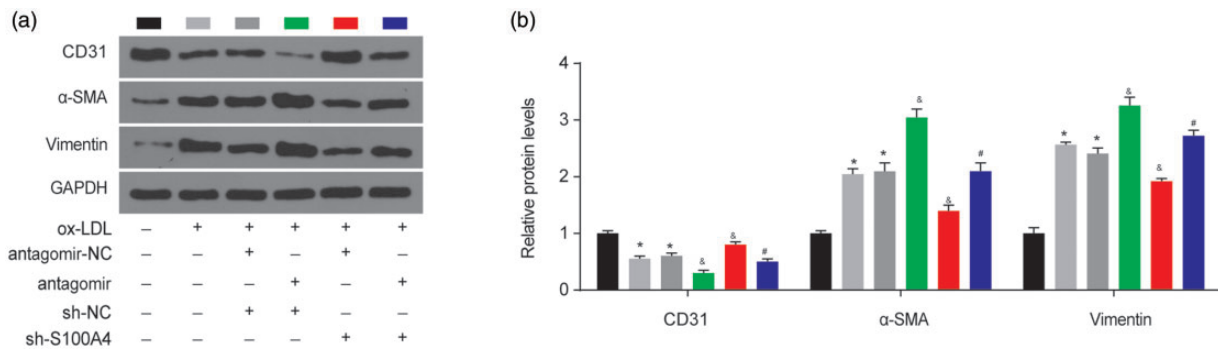


Figure 5. miR-296-5p/S100A4 axis regulates the EndMT in HUVECs. (a–b) The levels of CD31, α-SMA and vimentin were measured by Western blotting. **P* < 0.05 vs. Blank; &*P* < 0.05 vs. ox-LDL+antagonir-NC+sh-NC; #*P* < 0.05 vs. ox-LDL+antagonir+sh-NC. (A color version of this figure is available in the online journal.)

miR-296-5p/S100A4 axis participates in ox-LDL-induced endothelial-to-mesenchymal transition in HUVECs

As S100A4 is also considered a mesenchymal marker,^{11,12} we next examined the role of the miR-296-5p/S100A4 axis in the endothelial-to-mesenchymal transition (EndMT) in HUVECs. Endothelial markers (CD31) and mesenchymal markers (α-SMA and vimentin) were detected by Western blotting. As shown in Figure 5(a) and (b), after the ox-LDL treatment, the protein level of CD31 was downregulated,

and the α-SMA and vimentin protein levels were upregulated, confirming that ox-LDL induced the EndMT in the HUVECs. The miR-296-5p downregulation reduced the CD31 levels and increased the α-SMA and vimentin levels, suggesting that miR-296-5p inhibition promotes ox-LDL-induced EndMT in HUVECs. The S100A4 downregulation obviously increased the CD31 levels and decreased the α-SMA and vimentin levels, indicating that S100A4 inhibition recovers ox-LDL-induced EndMT. In addition, the ox-LDL-induced EndMT by the miR-296-5p

antagomir was restored by the S100A4 knockdown. These data indicate that the miR-296-5p/S100A4 axis is vital in ox-LDL-induced EndMT in HUVECs.

Decreased miR-296-5p participates in DVT formation in vivo

We further validated the effect of the miR-296-5p/S100A4 axis on DVT formation *in vivo*. Compared with the sham mice, the level of miR-296-5p was significantly reduced, and the level of S100A4 was enhanced in the vein tissue of the DVT mice. The miR-296-5p antagomir decreased miR-296-5p expression and enhanced the expression of

S100A4 in the DVT mice (Figure 6(a) and (b)). Thrombus organization was detected within the vessel cavity in the DVT group. The H&E staining showed that red-colored platelets, red cells, fibrin strands, and blue-colored nucleated cells, including ECs, monocytes, and neutrophil granulocytes, attached to the lining of the vein walls (Figure 6(c)). As expected, in the mice pretreated with the miR-296-5p antagomir, more blood clots were observed. In the mice pretreated with sh-S100A4, fewer blood clots were observed. Moreover, both the thrombus length and weight were greatly increased in the DVT miR-296-5p antagomir group and decreased in the DVT S100A4 knockdown groups (Figure 6(c) and (d)). The S100A4 knockdown

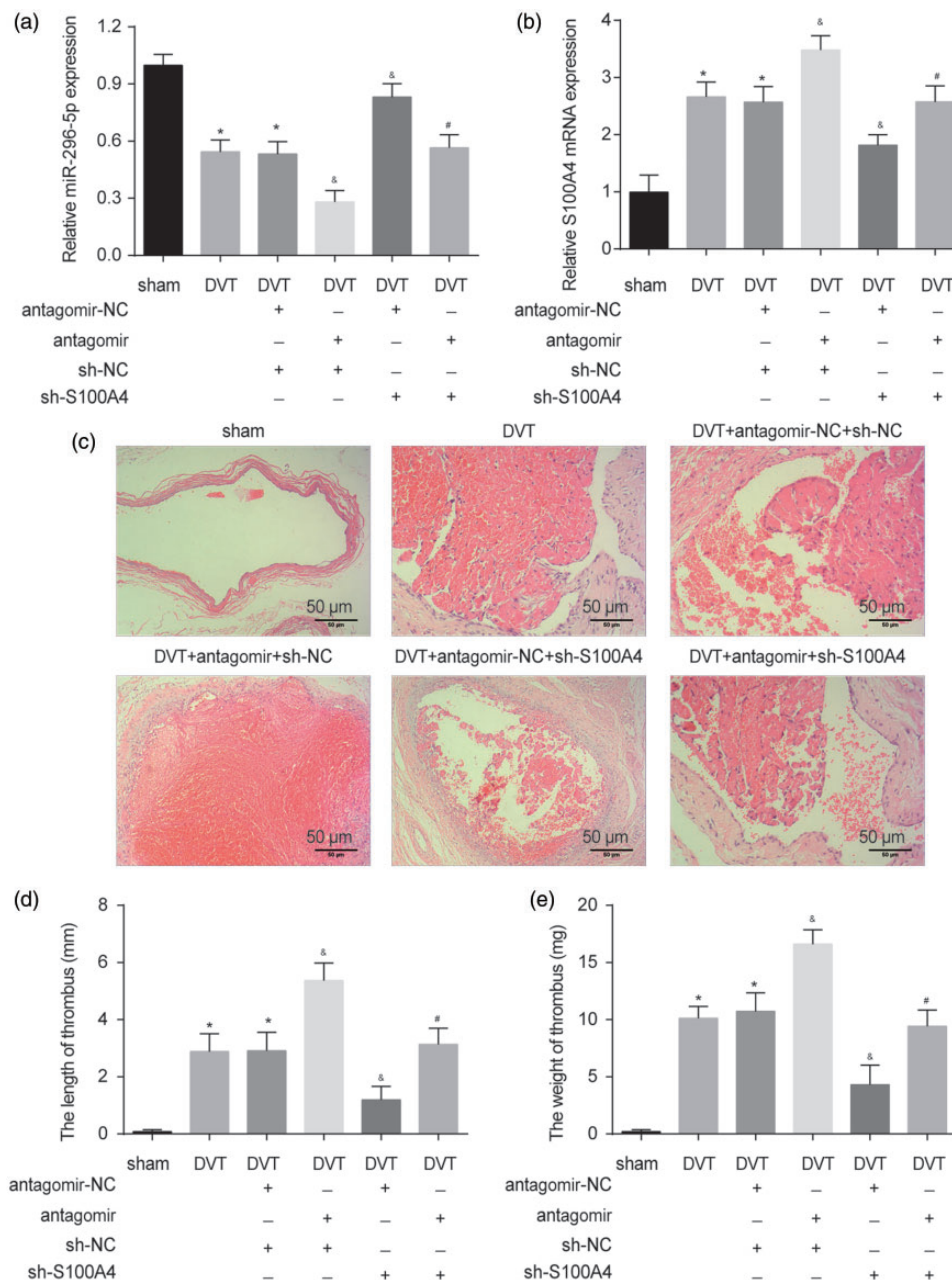


Figure 6. Role of the miR-296-5p/S100A4 axis in DVT formation. (a–b) The expression of miR-296-5p and S100A4 in vein tissue was detected by qRT-PCR. (c) H&E staining of IVCs from sham mice, DVT mice, and DVT mice treated with the miR-296-5p antagomir or sh-S100A4. (d–e) Thrombus length and weight of IVC ($n = 10$ per group). * $P < 0.05$ vs. sham; [§] $P < 0.05$ vs. DVT+antagomir-NC+sh-NC; [#] $P < 0.05$ vs. DVT+antagomir+sh-NC. (A color version of this figure is available in the online journal.)

reversed the positive effect of the miR-296-5p antagomir on DVT formation. Altogether, miR-296-5p regulated DVT formation *in vivo* by targeting S100A4.

miR-296-5p was increased and negatively correlated with S100A4 in DVT patients

The levels of miR-296-5p and the mRNA level of S100A4 in the venous blood of patients with and without DVT were detected. The results suggest that the DVT patients had a lower expression of miR-296-5p but a higher mRNA expression of S100A4 than the patients without DVT (Figure 7(a) and (b)). The Pearson's correlation analysis showed that miR-296-5p was negatively correlated with S100A4 in the DVT patients (Figure 7(c)). The ROC analysis revealed that miR-296-5p sensitively discriminated DVT in plasma with an area under the curve (AUC) of 0.88 (Figure 7(d)). S100A4 could also sensitively discriminate DVT in plasma with an AUC of 0.82 (Figure 7(e)). These data confirm that miR-296-5p and S100A4 are involved in DVT formation.

Discussion

In the present study, the miR-296-5p levels were found to be inhibited by ox-LDL in a dose-dependent manner in HUVECs. miR-296-5p knockdown could aggravate HUVEC injury induced by ox-LDL. S100A4 was found to be a direct target of miR-296-5p. The S100A4 knockdown abolished the harmful effect of the miR-296-5p antagomir in the ox-LDL-treated HUVECs and DVT mice. miR-296-5p regulated ox-LDL-induced apoptosis and ROS accumulation, prothrombosis-related factor expression, and the EndMT by inhibiting S100A4 in HUVECs. These findings

extend our understanding of the role of miRNAs in DVT, providing new targets for the diagnosis and treatment of DVT.

S100A4, which is also called FSP-1 (fibroblast-specific protein-1), is a fibroblast marker in the liver, kidney, heart, and lung undergoing tissue remodeling.¹³ S100A4 participates in a range of biological functions, such as cell apoptosis, differentiation, motility, and invasion.¹⁴ Moreover, S100A4 is closely related to inflammatory processes and oxidative stress.^{14,15} However, its role in DVT is rarely reported. Here, we found that S100A4 was enhanced in ox-LDL-stimulated HUVECs and that S100A4 knockdown reversed the ox-LDL-induced HUVEC injury by inhibiting apoptosis and ROS accumulation. Furthermore, S100A4 was found to have an effect on prothrombosis-related factor release and the EndMT in HUVECs. These data indicate that S100A4 may be a target for DVT treatment.

S100A4 can execute its function both intra- and extracellularly. Within the cell, S100A4 participates in apoptosis, migration, and the maintenance of cell stemness.^{16,17} Extracellular S100A4 can activate different processes by inducing the secretion of cytokines and matrix metalloproteinases and regulating inflammation-related pathways.^{18–20} In our study, we found that ox-LDL promoted the secretion of S100A4 (Figure S1). The miR-296-5p agomir inhibited the secretion of S100A4, and the miR-296-5p antagomir enhanced the secretion of S100A4 (Figure S1). These results indicate that miR-296-5p may play a role partially by regulating the secretion of S100A4 in HUVECs.

S100A4 is a biomarker of the EMT^{11,16,21} and a direct target of miR-296-5p. Therefore, miR-296-5p could regulate

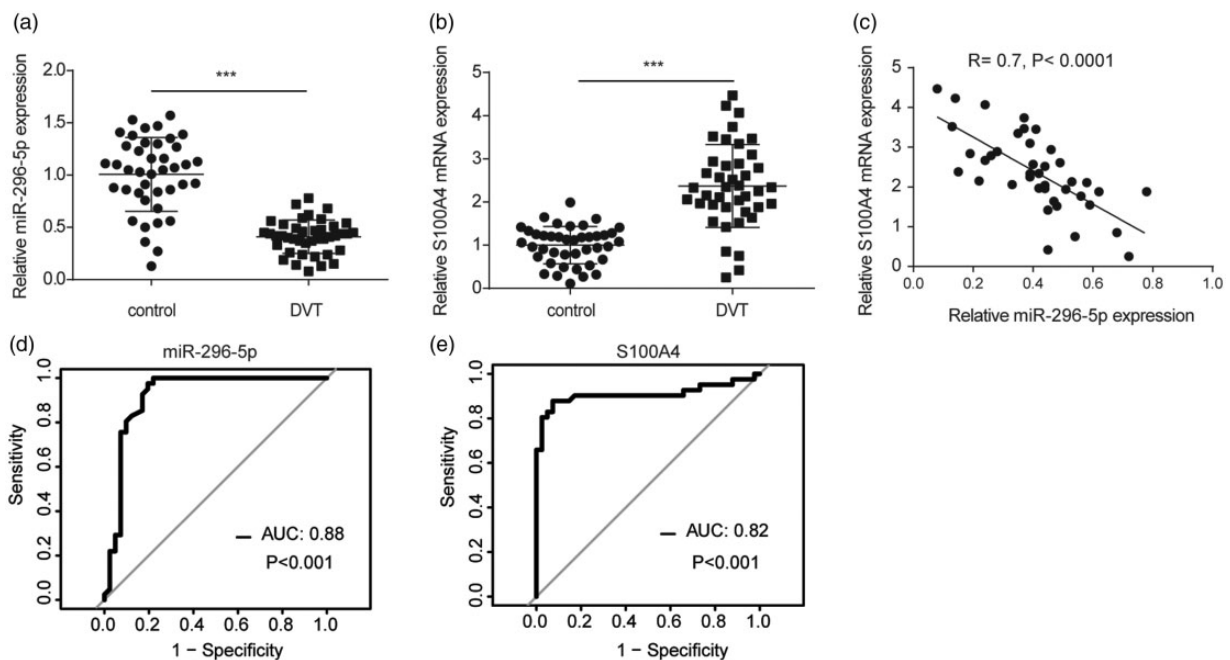


Figure 7. miR-296-5p was downregulated but S100A4 was enhanced in DVT patients. (a–b) The levels of miR-296-5p and S100A4 in patients with ($n = 41$) and without DVT ($n = 41$) were measured. *** $P < 0.001$. (c) The association between miR-296-5p expression and S100A4 expression was analyzed by a Pearson's correlation analysis of miR-296-5p and S100A4. (d) The diagnostic value of miR-296-5p for DVT was evaluated by a ROC curve analysis. (e) The diagnostic value of S100A4 for DVT was evaluated by a ROC curve analysis.

the EMT and change EMT-related gene expression through S100A4. In addition, some reports have indicated that miR-296-5p inhibits the EMT by targeting ZCCHC3 in osteosarcoma,²² targeting TGF- β in nasopharyngeal carcinoma,²³ and targeting the Akt2/SNAI1 signaling pathway in oral squamous cell carcinoma.²⁴ Furthermore, S100A4 is a key regulator of vascular remodeling.^{25,26} In our study, we found that the miR-296-5p antagomir promoted DVT *in vivo* and changed the ox-LDL-induced release of thrombosis-related factors in HUVECs *in vitro* through S100A4. These results indicate that miR-296-5p affects the EMT and thrombosis-related factor expression partially through S100A4.

Oxidative stress is an important cause of cardiovascular diseases, including DVT.²⁷ Dysfunctional endothelial cells (ECs) induced by oxidative stress induce a prothrombotic response by altering vasoconstriction and platelet aggregation and disrupting the balance of coagulation/anticoagulation and fibrinolysis/antifibrinolysis.¹⁰ The present study confirmed that the miR-296-5p/S100A4 axis treatment reversed ox-LDL-induced vascular endothelial cell oxidative stress injury. We also found that the miR-296-5p/S100A4 axis regulated pro-vasoconstriction protein (ET-1 and vWF) expression and pro-vasodilatation factor (NO and PGF1 α) secretion in ox-LDL-stimulated HUVECs. Therefore, our study supports a potential approach against DVT.

During embryonic development and disease progression, EC can transform into other cell types partially through the EndMT in which EC loses specific endothelial markers (CD31) and gradually expresses mesenchymal markers (α -SMA and vimentin).²⁸ The EndMT can be triggered by multiple pathological conditions, such as oxidative stress and inflammation, and can be observed in cardiac development, cardiac fibrosis, pulmonary hypertension, atherosclerosis, and thrombus formation.²⁹ The ox-LDL stimulation reduced CD31 expression and enhanced α -SMA and vimentin expression in HUVECs, indicating that ox-LDL promoted the EndMT in HUVECs. Altering miR-296-5p or S100A4 expression could change the EndMT in HUVECs induced by ox-LDL, suggesting that the miR-296-5p/S100A4 axis controls DVT progression partially by altering the EndMT of EC.

In conclusion, our study suggests that targeting the miR-296-5p/S100A4 axis antagonizes ox-LDL-induced HUVEC injury, thrombosis-related factor expression, and the EndMT. These findings highlight that the miR-296-5p/S100A4 axis may inhibit DVT progression by ameliorating vascular EC injury and the subsequent prothrombotic response, suggesting an underlying strategy for DVT.

AUTHORS' CONTRIBUTIONS

All authors participated in the design and interpretation of the studies, analysis of the data and review of the manuscript; ZCP, YZ, CYL, YY, RL, GFZ, WJF, QZ, ZYS, ZYG, JJR, and YYS conducted the experiments; ZCP, YZ, CYL, YY, RL, and GFZ supplied critical reagents; and ZCP, WJF, QZ, ZYS, ZYG, JJR, and YYS wrote the manuscript.

DECLARATION OF CONFLICTING INTERESTS

The author(s) declared no potential conflicts of interest with respect to the research, authorship, and/or publication of this article.

ETHICAL APPROVAL

The study was approved by the Ethics Committee of Suzhou TCM Hospital Affiliated to Nanjing University of Chinese Medicine. Informed consent was obtained from all individual participants included in this study.

FUNDING

The study was supported by the Youth Science and Technology Project of "Promoting Health through Science and Education" in Suzhou (Grant No: kxw2018039); the Science and Technology Project of Suzhou City of China (Grant No: SYSD2017179, SYSD2018154, SS2019071); the Fifth Batch of Health Personnel Training Project in Suzhou (Grant No: GSWS2019064); and the Advanced Research Fund in the Second Affiliated Hospital of Soochow University (Grant No: SDFEYJ1902).

ORCID ID

Jianjie Rong  <https://orcid.org/0000-0002-1201-8916>

SUPPLEMENTAL MATERIAL

Supplemental material for this article is available online.

REFERENCES

- Budnik I, Brill A. Immune factors in deep vein thrombosis initiation. *Trends Immunol* 2018;**39**:610–23
- Karande GY, Hedgire SS, Sanchez Y, Baliyan V, Mishra V, Ganguli S, Prabhakar AM. Advanced imaging in acute and chronic deep vein thrombosis. *Cardiovasc Diagn Ther* 2016;**6**:493–507
- Zhou X, Liu H, Zheng Y, Han Y, Wang T, Zhang H, Sun Q, Li Z. Overcoming radioresistance in tumor therapy by alleviating hypoxia and using the HIF-1 inhibitor. *ACS Appl Mater Interfaces* 2020;**12**:4231–40
- Zhu L, Cheng J, Gu P, Liu Y, Liu J, Wang J, Shen H. Therapeutic strategies of thromboembolic events in patients with inflammatory bowel diseases: two case reports. *Medicine* 2019;**98**:e14622
- Zhang Y, Zhang Z, Wei R, Miao X, Sun S, Liang G, Chu C, Zhao L, Zhu X, Guo Q, Wang B, Li X. IL (interleukin)-6 contributes to deep vein thrombosis and is negatively regulated by miR-338-5p. *Arterioscler Thromb Vasc Biol* 2020;**40**:323–34
- Yang N, Zhu S, Lv X, Qiao Y, Liu YJ, Chen J. MicroRNAs: pleiotropic regulators in the tumor microenvironment. *Front Immunol* 2018;**9**:2491
- Jiang Z, Ma J, Wang Q, Wu F, Ping J, Ming L. Circulating microRNA expression and their target genes in deep vein thrombosis: a systematic review and bioinformatics analysis. *Medicine* 2017;**96**:e9330
- Zhang E, Wu Y. MicroRNAs: important modulators of oxLDL-mediated signaling in atherosclerosis. *J Atheroscler Thromb* 2013;**20**:215–27
- Diaz JA, Obi AT, Myers DD, Jr., Wroblewski SK, Henke PK, Mackman N, Wakefield TW. Critical review of mouse models of venous thrombosis. *Arterioscler Thromb Vasc Biol* 2012;**32**:556–62
- Poredos P, Jezovnik MK. Endothelial dysfunction and venous thrombosis. *Angiology* 2018;**69**:564–7
- Tochimoto M, Oguri Y, Hashimura M, Konno R, Matsumoto T, Yokoi A, Kodera Y, Saegusa M. S100A4/non-muscle myosin II signaling

- regulates epithelial-mesenchymal transition and stemness in uterine carcinosarcoma. *Lab Invest* 2020;**100**:682–95
12. Piera-Velazquez S, Jimenez SA. Endothelial to mesenchymal transition: role in physiology and in the pathogenesis of human diseases. *Physiol Rev* 2019;**99**:1281–324
 13. Fernandez IE, Eickelberg O. New cellular and molecular mechanisms of lung injury and fibrosis in idiopathic pulmonary fibrosis. *Lancet* 2012;**380**:680–8
 14. Ambartsumian N, Klingelhofer J, Grigorian M. The multifaceted S100A4 protein in cancer and inflammation. *Methods Mol Biol* 2019;**1929**:339–65
 15. Indo HP, Matsui H, Chen J, Zhu H, Hawkins CL, Davies MJ, Yarana C, St Clair DK, Majima HJ. Manganese superoxide dismutase promotes interaction of actin, S100A4 and talin, and enhances rat gastric tumor cell invasion. *J Clin Biochem Nutr* 2015;**57**:13–20
 16. Chow KH, Park HJ, George J, Yamamoto K, Gallup AD, Graber JH, Chen Y, Jiang W, Steindler DA, Neilson EG, Kim BYS, Yun K. S100A4 is a biomarker and regulator of glioma stem cells that is critical for mesenchymal transition in glioblastoma. *Cancer Res* 2017;**77**:5360–73
 17. Dahlmann M, Kobelt D, Walther W, Mudduluru G, Stein U. S100A4 in cancer metastasis: Wnt signaling-driven interventions for metastasis restriction. *Cancers* 2016;**8**:59
 18. Elenjord R, Ljones H, Sundkvist E, Loennechen T, Winberg JO. Dysregulation of matrix metalloproteinases and their tissue inhibitors by S100A4. *Connect Tissue Res* 2008;**49**:185–8
 19. Rud AK, Lund-Iversen M, Berge G, Brustugun OT, Solberg SK, Maelandsmo GM, Boye K. Expression of S100A4, ephrin-A1 and osteopontin in non-small cell lung cancer. *BMC Cancer* 2012;**12**:333
 20. Senolt L, Grigorian M, Lukanidin E, Simmen B, Michel BA, Pavelka K, Gay RE, Gay S, Neidhart M. S100A4 is expressed at site of invasion in rheumatoid arthritis synovium and modulates production of matrix metalloproteinases. *Ann Rheum Dis* 2006;**65**:1645–8
 21. Nader JS, Guillon J, Petit C, Boissard A, Franconi F, Blandin S, Lambot S, Gregoire M, Verrielle V, Nawrocki-Raby B, Birembaut P, Coqueret O, Guette C, Pouliquen DL. S100A4 is a biomarker of tumorigenesis, EMT, invasion, and colonization of host organs in experimental malignant mesothelioma. *Cancers* 2020;**12**:939
 22. Wang L. ELF1-activated FOXD3-AS1 promotes the migration, invasion and EMT of osteosarcoma cells via sponging miR-296-5p to upregulate ZCCHC3. *J Bone Oncol* 2021;**26**:100335
 23. Chen M, Chen C, Luo H, Ren J, Dai Q, Hu W, Zhou K, Tang X, Li X. MicroRNA-296-5p inhibits cell metastasis and invasion in nasopharyngeal carcinoma by reversing transforming growth factor-beta-induced epithelial-mesenchymal transition. *Cell Mol Biol Lett* 2020;**25**:49
 24. Zhang S, Li C, Liu J, Geng F, Shi X, Li Q, Lu Z, Pan Y. Fusobacterium nucleatum promotes epithelial-mesenchymal transition through regulation of the lncRNA MIR4435-2HG/miR-296-5p/Akt2/SNAI1 signaling pathway. *FEBS J* 2020;**287**:4032–47
 25. Nagata M, Minami M, Yoshida K, Yang T, Yamamoto Y, Takayama N, Ikedo T, Hayashi K, Miyata T, Yokode M, Miyamoto S. Calcium-binding protein S100A4 is upregulated in carotid atherosclerotic plaques and contributes to expansive remodeling. *J Am Heart Assoc* 2020;**9**:e016128
 26. Furmanik M, Chatrou M, van Gorp R, Akbulut A, Willems B, Schmidt H, van Eys G, Bochaton-Piallat ML, Proudfoot D, Biessen E, Hedin U, Perisic L, Mees B, Shanahan C, Reutelingsperger C, Schurgers L. Reactive oxygen-forming Nox5 links vascular smooth muscle cell phenotypic switching and extracellular vesicle-mediated vascular calcification. *Circ Res* 2020;**127**:911–27
 27. Ekim M, Sekeroglu MR, Balahoroglu R, Ozkol H, Ekim H. Roles of the oxidative stress and ADMA in the development of deep venous thrombosis. *Biochem Res Int* 2014;**2014**:703128
 28. Zeisberg EM, Tarnavski O, Zeisberg M, Dorfman AL, McMullen JR, Gustafsson E, Chandraker A, Yuan X, Pu WT, Roberts AB, Neilson EG, Sayegh MH, Izumo S, Kalluri R. Endothelial-to-mesenchymal transition contributes to cardiac fibrosis. *Nat Med* 2007;**13**:952–61
 29. Hong L, Du X, You T, Sun L, Li W, Xiao L, Lu H, Wang W, Li X. Reciprocal enhancement of thrombosis by endothelial-to-mesenchymal transition induced by iliac vein compression. *Life Sci* 2019;**233**:116659

(Received February 7, 2021, Accepted May 17, 2021)